Manuscript type: Original paper

Title:

Tumour texture features from preoperative CT predict high-risk disease in endometrial cancer.

Highlights

- High tumour entropy predicts deep myometrial invasion and cervical stroma invasion.
- High tumour kurtosis predicts reduced recurrence- and progression-free survival.
- Texture analysis may enhance the role of standard diagnostic imaging methods.

Abstract

BACKGROUND

To enable more individualised treatment of endometrial cancer, improved methods for preoperative tumour characterization are warranted. Texture analysis is a method for quantification of heterogeneity in images, increasingly reported as a promising diagnostic tool in oncological imaging, but largely unexplored in endometrial cancer

AIM

To explore whether tumour texture features from preoperative computed tomography (CT) are related to known prognostic histopathological features and to outcome in endometrial cancer patients.

MATERIALS AND METHODS

Preoperative pelvic contrast-enhanced CT was performed in 155 patients with histologically confirmed endometrial cancer. Tumour ROIs were manually drawn on the section displaying the largest cross-sectional tumour area, using dedicated texture analysis software. Using the filtration-histogram technique, the following texture features were calculated: mean, standard deviation, entropy, mean of positive pixels (MPP), skewness, and kurtosis. These imaging markers were evaluated as predictors of histopathological high-risk features and recurrence- and progression-free survival using multivariable logistic regression and Cox regression analysis, including models adjusting for high-risk status based on preoperative biopsy, magnetic resonance imaging (MRI) findings, and age.

RESULTS

High tumour entropy independently predicted deep myometrial invasion (odds ratio [OR] 3.7, p=0.008) and cervical stroma invasion (OR 3.9, p=0.02). High value of MPP (MPP5 >24.2) independently predicted high-risk histological subtype (OR 3.7, p=0.01). Furthermore, high tumour kurtosis tended to independently predict reduced recurrence- and progression-free survival (HR 1.1, p=0.06).

CONCLUSION

CT texture analysis yields promising imaging markers in endometrial cancer and may supplement other imaging techniques in providing a more refined preoperative risk assessment that may ultimately enable better tailored treatment strategies.

Introduction

Intratumour heterogeneity at the genetic or histological level is reportedly a driver of carcinogenesis, neoplastic progression and therapeutic resistance (1-4). In the diagnostic workup of most cancer types, imaging is an important cornerstone, providing non-invasive, high resolution, whole-tumour visualisation. In recent years, assessment of tumour image heterogeneity has provided important insights into tumour phenotype, and several risk stratification tools based on radiomics have been proposed (5).

Endometrial cancer is the most common gynaecological malignancy in developed countries, and the incidence is reported to be increasing (6). The current staging system, revised by the International Federation of Gynecology and Obstetrics (FIGO) in 2009 (7) is surgical, which implies that prognostication is largely based on results from primary surgical staging, thus after the surgical treatment. Hysterectomy with bilateral salpingo-oophorectomy comprises the standard primary surgical treatment. Pelvic and/or para-aortic lymphadenectomy is additionally performed in selected patients according to guidelines varying between institutions. The depth of myometrial and cervical tumour invasion, as well as the histological type and grade, are established markers associated with presence of lymph node metastases, post-treatment recurrence and patient survival (8). If these parameters could be accurately predicted preoperatively, a shift towards preoperative decision-making would be facilitated. In general, to enable more individualised surgical treatment and to avoid surgical overtreatment, improved methods for preoperative risk stratification are warranted.

Magnetic resonance imaging (MRI) is widely used for preoperative pelvic assessment of endometrial cancer (9-11). Additionally, most patients undergo an abdominal and thoracic computed tomography (CT) scan as part of the routine preoperative diagnostic workup. Some institutions also include 18-fluoro-deoxy-glucose (FDG)-positron-emission tomography (PET) in preoperative assessments, due to its high diagnostic value in detecting lymph node metastases

(12). Texture analysis, a method for quantification of heterogeneity in images which is applicable to both MRI, PET and CT, is increasingly employed in clinical research. As a post-processing tool, image texture analysis does not increase scan time or patient-related side effects e.g. radiation dose, and thus represents an intriguing adjunct to conventional imaging. Image texture features have been proposed as imaging markers yielding more accurate diagnosis, improved preoperative risk stratification and better assessment of treatment response in several cancer types, e.g. in the brain (13), lung (14), breast (15) and prostate (16). Recent publications also report texture analysis of MRI (17, 18) and PET (19) as promising tools for preoperative risk stratification in endometrial cancer. No prior study has evaluated the possible value of CT texture analysis (CTTA) in endometrial cancer.

This study aimed to explore whether the staging parameters pathological deep (≥50%) myometrial invasion (pDMI), cervical stroma invasion (pCSI) and lymph node metastases (pLNM), high-risk histological subtype and clinical outcome in endometrial cancer patients, are reflected in CTTA features.

Materials and Methods

Study setting

This study was conducted with written informed consent from all patients and approval by the regional ethics committee. From April 2009 to November 2013 preoperative pelvic contrast-enhanced CT (ceCT) was performed in 155 women with endometrial cancer histologically verified at subsequent surgical staging. The CT scans were performed at different local hospitals. All patients were treated at the same university hospital, which is a European Society of Gynaecological Oncology accredited center. The last follow-up was in January 2017

and median follow-up time for the group of patients without recurrence or progression was 50 months (range 0-85).

Histological diagnosis

Mean interval between the CT examination and surgical staging was 7 (range 1-102) days. The preoperative biopsy was graded as either low-risk (endometrioid grade 1-2) or high-risk (endometrioid grade 3 or non-endometrioid) endometrial cancer. From preoperative endocervical curettage, an assessment of cervical tumour involvement was also performed.

All patients were surgicopathologically staged according to the 2009 FIGO staging system (7). Hysterectomy specimens were sectioned along the longitudinal plane of the uterus, and myometrial invasion and cervical stroma invasion were estimated grossly and confirmed microscopically according to standard criteria (20). In this paper we use the notation pDMI, pCSI and pLNM to indicate surgicopathological staging results, as opposed to imaging findings (e.g. iDMI indicating presence of ≥50% myometrial invasion on MRI).

Imaging protocol

CT was performed on different scanners at different local hospitals in Western Norway. Imaging data have been retrospectively collected, and thus, were not acquired using a standardised protocol. However, all patients underwent ceCT in a routine clinical setting as part of the diagnostic workup of endometrial cancer. Only portovenous contrast phase images acquired with diagnostic CT radiation dose and reconstructed with a soft tissue algorithm were considered eligible for the study. All patients had CT images reconstructed in axial, coronal and sagittal plane, aligned to the body axis (not to the long axis of the uterus). Section thickness was consistently 3 mm, in-plane resolution ranged from 0.65×0.65 mm^2 to 1.06×1.06 mm^2.

Image analysis

A previously published study on MRI texture analysis (18) included 180 endometrial cancer patients. This MRI study was prospective with a standardised scan protcol based on guidelines from the European Society of Urogenital Imaging (ESUR) (10). In 169 of these 180 patients, a pelvic ceCT was available. One radiologist (SYH) with 6 years of experience with pelvic CT and MR imaging, blinded for clinical and histological data, assessed the eligibility of the images for CTTA. Of the 169 patients with a ceCT, 14 were excluded due to poorly defined tumours, considered ineligible for reliable tumour texture analysis. Thus, 155 patients were included for CTTA. Aiming at selecting the image series best approximating a true cross-sectional tumour plane, axial or coronal (depending on the degree of ante-/retroflection of the uterus) ceCT images were exported to the commercially available research software TexRAD (TexRAD Ltd, part of Feedback Plc). Then, the image slice displaying the largest cross-sectional tumour area was selected for texture analysis. In cases with several candidate slices, the radiologist subjectively selected one single slice based on the criteria large tumour area, good image quality and high tumour-background contrast. Median number of pixels in regions of interest (ROIs) was 466 (range 53-7541).

Texture analysis

In TexRAD the radiologist (SYH) manually drew ROIs on the CT slice displaying the largest cross-sectional tumour area, aiming at including all viable tumour tissue (Figure 1). To optimise tumour segmentation, MR images (T2-weighted, diffusion weighted and contrast enhanced T1-weighted images) were available when drawing ROIs on CT images (Suppl. Figure 1AB). The ROIs were processed using a filtration-histogram technique (21), in which image elements, i.e. groups of pixels with similar density, of different sizes were enhanced corresponding to spatial scale filter (SSF) from 2-6 mm, i.e. fine (2 mm), medium (3-5 mm)

and coarse texture (6 mm) (Figure 1). Quantification of texture in tumour ROIs comprised mean density, standard deviation (SD), entropy, mean of positive pixels (MPP), skewness and kurtosis. The total number of texture variables included in the statistical analyses was 36 (mean/SD/entropy/skewness/MPP/kurtosis at SSF 0/2/3/4/5/6). A condensed notation is used in this manuscript, e.g. Entropy6, indicating tumour ROI entropy in ceCT image at SSF 6. The additional time consume for image slice selection and export, tumour delineation and texture analysis was approximately 10-15 minutes per patient.

Statistical analysis

The majority of texture variables did not have normal distribution, thus non-parametric tests were chosen. Mann-Whitney U Test was used to evaluate associations between tumour texture variables and the pathological outcome variables pDMI, pCSI, pLNM and high-risk histological subtype (defined as endometrioid grade 3 or non-endometrioid). The texture variables were subsequently ranked according to lowest p-value, and the highest ranked variables were selected for receiver operator characteristic (ROC)-curve analyses and univariable and multivariable logistic regression. The selected texture variables were analysed both as continuous and categorical variables. To generate the categorical variables, cutoff values determined by the maximum Youden index (defined as the sum of sensitivity and specificity) were used. In the multivariable analyses, we adjusted for age, preoperative biopsy risk status and conventional MRI reading results including MRI-measured tumour volume. Results from conventional MRI (assessment of tumour size, myometrial (iDMI) and cervical invasion (iCSI) and presence of lymph node metastases (iLNM)) were recorded as consensus opinion from three radiologists (median values for continuous variables and majority for categorical variables) having independently read the same MR images in a prior study (22).

Spearman's bivariate correlation test was used to explore correlations.

Survival analysis was performed with all texture variables separately in univariable Cox regression analysis for predicting recurrence- and progression-free survival (RPFS), i.e. time to recurrence (for patients considered to be cured by primary treatment) or progression (for patients known to have residual disease after primary treatment). Ranked according to lowest p-value, the best predictor was selected to be included in a multivariable analysis also including MRI-measured tumour volume, preoperative biopsy risk status and age. For the top ranked texture variable, difference in RPFS was assessed by the Mantel-Cox test and Kaplan-Meier plot, in which consecutive groups (quartiles) with similar survival were merged.

For the testing of the 36 texture variables, an adjustment for inter-variable correlations (Suppl. Table 1) was done and the significance level was set to 0.0025. With this significance level for the 36 individual tests, a random allocation (without replacement) of the 36-variate texture variables to outcome group had approximately 5% chance of at least one significant result.

In the multivariable analyses a traditional significance level of 0.05 was used.

The data were analysed using SPSS 24.0 (IBM, Armonk, NY, USA).

Results

Patients

Median patient age at primary treatment in the study cohort (n=155) was 68 years (range 41-89). Primary surgical treatment included bilateral salpingo-oophorectomy and hysterectomy for 98% (152/155), tumour reduction surgery for 1/155 and curettage only for 2/155. Lymphadenectomy was performed in 85% (131/155), pelvic only in 105 patients, pelvic and para-aortic in 26 patients. In patients who underwent lymphadenectomy, the mean number of resected nodes was 17 (range 1-54). FIGO stage was IA in 47% (73/155), IB in 27% (42/155),

II in 10% (16/155), IIIB in 2% (3/155), IIIC1 in 7% (11/155), IIIC2 in 4% (6/155), IVA in 1% (1/155) and IVB in 2% (3/155). Histological subtype was endometrioid in 78% (121/155), clear cell in 3% (5/155), serous in 10% (16/155), carcinosarcoma in 6% (9/155) and undifferentiated/others in 3% (4/155). Among endometrioid tumours, histological differentiation was grade 1 in 43% (52/121), grade 2 in 32% (39/121), grade 3 in 23% (28/121) and ungraded in 2% (2/121). Adjuvant therapy was given to 41% (63/155); comprising chemotherapy in 54 patients, radiotherapy (external or internal) in 8 patients and hormonal treatment in 1 patient.

Prediction of deep myometrial invasion (pDMI)

Of the 36 texture features assessed, 15 significantly ($p<0.0025$) predicted pDMI in univariable analysis with entropy at filter level 6 (Entropy6) yielding highest significance (Suppl. Table 2 and 3). The majority of these features comprised entropy and kurtosis at various filter levels, yielding the top 6 significant predictors (Suppl. Table 3). High values for Entropy6 independently predicted pDMI with an odds ratio (OR) of 3.7 (95% confidence interval 1.4-9.7, $p=0.008$) when adjusting for high-risk status based on preoperative biopsy (endometrioid grade 3 or non-endometrioid), conventional MRI reading suggesting iDMI, MRI-measured tumour volume and age (Table 1). The receiver operator characteristic (ROC)-analysis yielded an area under the Entropy6 ROC-curve (AU-ROC) of 0.71 ($p<0.001$) (Figure 2a) for prediction of pDMI.

Prediction of cervical stroma invasion (pCSI)

For prediction of pCSI in univariable analysis, none of the 36 texture features reached the significance level of 0.0025. The top ranked predictor of pCSI, Entropy6 (also the best predictor of pDMI), was, however, borderline significant in univariable analysis ($p=0.006$),

whereas in the multivariable analysis (significance level 0.05) high values of Entropy6 independently predicted pCSI with an odds ratio of 3.9 (1.2-12.4, p=0.02) when adjusting for preoperative endocervical curettage indicating cervical tumour invasion, conventional MRI reading suggesting iCSI, MRI-measured tumour volume and age (Table 1). The corresponding AU-ROC for Entropy6 was 0.67 (p=0.005) (Figure 2b) for prediction of pCSI.

Prediction of lymph node metastases (pLNM)

None of the 36 texture features were significant predictors of pLNM neither in univariable analysis nor in multivariable analysis. The top ranked feature, Kurtosis5, yielded an AU-ROC of 0.69 (p=0.01) (Figure 2c) for prediction of pLNM.

Prediction of high-risk histological subtype

Two of the tested 36 texture features, MPP5 and Entropy4, were significant ($p<0.0025$) predictors of high-risk histological subtype (endometrioid grade 3 and non-endometrioid tumours) in univariable analysis (Suppl. Table 2 and 3). In the multivariable analysis, high values of the top ranked predictor, MPP5, only tended to predict high-risk histological subtype (OR 1.01 (1.00-1.03, p=0.10)) when adjusting for high-risk status based on preoperative biopsy, MRI-measured tumour volume and age (Table 1). However, when a cutoff based on the highest Youden index was applied, MPP5>24.2 independently predicted high-risk histological subtype in the same multivariable model (OR 3.7 (1.3-10.1, p=0.01)). The corresponding AU-ROC for MPP5 was 0.65 (p=0.002) (Figure 2d) for prediction of high-risk histological subtype.

Survival analysis

Three out of 36 texture features significantly ($p<0.0025$) predicted recurrence- and progression-free survival (RPFS) in univariable Cox regression analysis. These comprised kurtosis at filter level 5, 4 and 3, respectively (Suppl. Table 3). High values of the top ranked prognostic texture feature, Kurtosis5 (also the best predictor of pLNM), predicted reduced survival with a hazard ratio of 1.2 (1.1-1.2, $p<0.001$) in univariable analysis (Table 2). When adjusted for high-risk status based on preoperative biopsy, MRI-measured tumour volume and age, however, the significance was only borderline ($p=0.06$).

Significantly reduced recurrence- and progression-free survival was observed for patients with Kurtosis5 value being above the 75-percentile compared with patients having Kurtosis5 value below the 75-percentile (Figure 3, $p<0.001$). The proportion of patients given adjuvant treatment was higher in the poor outcome group: 59% (23/39) received adjuvant treatment among patients with Kurtosis5 above the 75-percentile, whereas only 34% (40/116) received adjuvant treatment among patients with Kurtosis5 below the 75-percentile.

Discussion

In this study we have demonstrated that texture features derived from preoperative CT are associated with high-risk disease and reduced survival in endometrial cancer. Our findings suggest that tumour texture analysis also employed on CT scans may yield clinically relevant imaging markers that may aid in the preoperative staging and risk assessment.

Surgical staging and subsequent histological assessment have traditionally been the primary basis for treatment and prognostication in endometrial cancer, thereby allowing only limited risk stratification prior to surgery. In this study we link novel CT features that may be derived from routinely employed preoperative scanning, to established risk factors in endometrial cancer, and identify tumour texture features that non-invasively and accurately may predict high-risk disease preoperatively. Interestingly, in multivariable analyses when

adjusting for other relevant routinely obtained preoperative biomarkers, the texture feature Entropy6 remains a significant and independent predictor of both pDMI and pCSI. Furthermore, in the multivariable survival analysis, the texture feature Kurtosis5 tends to predict recurrence- and progression-free survival.

Among the CT derived texture features in this study we found entropy, kurtosis and to some extent MPP to be the most promising markers in endometrial cancer. These findings are in concordance with a prior endometrial cancer study applying texture analysis on MRI with a similar approach (18). Entropy is a measure of random irregularity and kurtosis is related to the peakedness of the pixel distribution curve in ROIs. In general, high entropy and high kurtosis in CT images reflect increased histological heterogeneity (23), which in turn is often related to irregular tissue architecture induced by tumour-induced angiogenesis, hypoxia and necrosis (24). Although texture features at different filter levels in our study are highly correlated (Suppl. Table 1), there is a tendency towards medium to coarse filtration being more frequently represented among high ranked predictors of high-risk disease (Suppl. Table 3). This observation may support that the filtering-algorithm in TexRAD in fact enhances the biologically relevant information in medical images, as hypothesised (25).

Inherently, CT has a lower soft tissue contrast than MRI, and in endometrial cancer CT has traditionally played a limited role in the assessment of local tumour extent. Although not fully comparable, a previous study with overlapping patient cohort employing MR texture analysis (MRTA) (18), identified features yielding slightly higher predictive and prognostic value than the most significant CTTA features in the present study. The MRTA markers yielded higher AUC than CTTA for prediction of pDMI (ADC_Entropy6 0.81 versus CT_Entropy6 0.71), pLNM (T1c_Entropy6 0.73 versus CT_ Kurtosis5 0.69) and high-risk histological subtype (T1c_MPP4 0.66 versus CT_MPP5 0.65) and higher hazard ratio (1.5 for T1c_Kurtosis2 versus 1.1 for CT_Kurtosis5) for predicting recurrence- and progression-free

survival. Nevertheless, the current study demonstrates that in spite of the lower soft tissue contrast, CT derived texture features may aid in the preoperative risk assessment as an adjunct to MRI. In fact, for prediction of pCSI, CTTA yielded slightly higher AUC than MRTA (CT_Entropy6 0.67 versus T2_MPP4 0.64), and if MRI is not available, the role of CTTA may potentially be even more important. In this context, however, it should be noted that our study allowed corresponding MR images to assist in tumour segmentation (to minimise ROI contamination) and as such, further studies are required to evaluate CTTA as a standalone prognosticator. Furthermore, our study does not propose a complete risk predicting model for endometrial cancer. However, given the previously published results on image texture analysis of MRI (17, 18) and PET (19), it seems plausible that a "texture signature", including features from different imaging modalities, could improve preoperative risk stratification in endometrial cancer patients.

The presence of lymph node metastases at surgical staging is an important risk classifier. In this study CTTA does not independently predict pLNM. A prior MRTA study also failed to identify independent predictors of pLNM among 87 texture features (18). Preoperative biomarkers for prediction of pLNM need to yield high diagnostic performance if these biomarkers are to guide tailored surgical treatment strategies offering less invasive surgery in low-risk patients. It is worth noting that aggressive disease does not always present with macroscopic lymph node metastases at the time of diagnosis or staging. Thus, if imaging can provide accurate prediction of pDMI, pCSI and histological type and grade, this would also be an important contribution to preoperative risk stratification. Anyhow, since no single promising texture marker for prediction of pLNM is currently identified, a future risk prediction model would probably benefit from a more multimodal and integrative approach, tentatively including elements from biopsy specimen (histological and molecular markers), blood sample, radiology and clinical information.

Our study has some limitations. First, the CT images were acquired using a non-standardised imaging protocol, and hence the heterogeneous dataset represents a potential bias. E.g. differences in the quantities and types of contrast media administered may have had an impact on the derived image texture features. This, however, primarily increases the risk of type II errors, and our findings of independent predictors of high-risk disease could thus be regarded even more robust, as they are based on imaging data from routine clinical practice. Second, intra- and interobserver variability for the texture measurements has not been assessed in this study, in which manual segmentation was performed. Although not directly comparable, prior CTTA studies using the same software in other cancer types have shown good to excellent interobserver agreement (26, 27).

Third, the two-dimensional, filtration-histogram based approach in TexRAD does not cover all aspects of texture analysis, and a three-dimensional approach analysing the entire tumour volume could potentially have yielded more relevant information on tumour texture. The literature is, however, equivocal regarding the superiority of whole tumour volume texture analysis over largest cross-sectional tumour area texture analysis. Studies on CT texture analysis in colorectal cancer yielded similar results for 2D and 3D segmentation of liver metastases (28), whereas for primary tumours the 3D segmentation yielded slightly better prognostic markers than that based on 2D segmentation (29). Since 2D segmentation is less time consuming, it is still widely used; however, with the introduction of more automated tumour segmentation tools, whole volume texture analyses may be easier to conduct in the future.

In conclusion, preoperative tumour texture analysis from CT yields imaging markers that independently predict high-risk disease and tend to predict reduced survival in endometrial cancer patients. This approach using radiomics to yield prognostic markers may enhance the role of standard diagnostic imaging methods and potentially contribute to

preoperative risk stratification in endometrial cancer. However, the value of image texture analysis in endometrial cancer needs to be further evaluated and validated across observers, centers and platforms, prior to potential implementation in clinic.

Reference List

1. Andor N, Graham TA, Jansen M, et al. Pan-cancer analysis of the extent and consequences of intratumor heterogeneity. Nat Med 2016;22:105-113.

2. Morris LG, Riaz N, Desrichard A, et al. Pan-cancer analysis of intratumor heterogeneity as a prognostic determinant of survival. Oncotarget 2016;7:10051-10063.

3. Gerlinger M, Rowan AJ, Horswell S, et al. Intratumor heterogeneity and branched evolution revealed by multiregion sequencing. N Engl J Med 2012;366:883-892.

4. Yates LR, Gerstung M, Knappskog S, et al. Subclonal diversification of primary breast cancer revealed by multiregion sequencing. Nat Med 2015;21:751-759.

5. Sala E, Mema E, Himoto Y, et al. Unravelling tumour heterogeneity using next-generation imaging: radiomics, radiogenomics, and habitat imaging. Clin Radiol 2017;72:3-10.

6. Amant F, Moerman P, Neven P, Timmerman D, Van LE, Vergote I. Endometrial cancer. Lancet 2005;366:491-505.

7. Pecorelli S. Revised FIGO staging for carcinoma of the vulva, cervix, and endometrium. Int J Gynaecol Obstet 2009;105:103-104.

8. Morice P, Leary A, Creutzberg C, Abu-Rustum N, Darai E. Endometrial cancer. Lancet 2016;387:1094-1108.

9. Frei KA, Kinkel K. Staging endometrial cancer: role of magnetic resonance imaging. J Magn Reson Imaging 2001;13:850-855.

10. Kinkel K, Forstner R, Danza FM, et al. Staging of endometrial cancer with MRI: guidelines of the European Society of Urogenital Imaging. Eur Radiol 2009;19:1565-1574.

11. Sala E, Rockall AG, Freeman SJ, Mitchell DG, Reinhold C. The added role of MR imaging in treatment stratification of patients with gynecologic malignancies: what the radiologist needs to know. Radiology 2013;266:717-740.

12. Bollineni VR, Ytre-Hauge S, Bollineni-Balabay O, Salvesen HB, Haldorsen IS. High Diagnostic Value of 18F-FDG PET/CT in Endometrial Cancer: Systematic Review and Meta-Analysis of the Literature. J Nucl Med 2016;57:879-885.

13. Rose CJ, Mills SJ, O'Connor JP, et al. Quantifying spatial heterogeneity in dynamic contrast-enhanced MRI parameter maps. Magn Reson Med 2009;62:488-499.

14. Ganeshan B, Goh V, Mandeville HC, Ng QS, Hoskin PJ, Miles KA. Non-small cell lung cancer: histopathologic correlates for texture parameters at CT. Radiology 2013;266:326-336.

15. Ahmed A, Gibbs P, Pickles M, Turnbull L. Texture analysis in assessment and prediction of chemotherapy response in breast cancer. J Magn Reson Imaging 2013;38:89-101.

16. Wibmer A, Hricak H, Gondo T, et al. Haralick texture analysis of prostate MRI: utility for differentiating non-cancerous prostate from prostate cancer and differentiating prostate cancers with different Gleason scores. Eur Radiol 2015;25:2840-2850.

17. Ueno Y, Forghani B, Forghani R, et al. Endometrial Carcinoma: MR Imaging-based Texture Model for Preoperative Risk Stratification-A Preliminary Analysis. Radiology 2017;284:748-757.

18. Ytre-Hauge S, Dybvik JA, Lundervold A, et al. Preoperative tumor texture analysis on MRI predicts high-risk disease and reduced survival in endometrial cancer. J Magn Reson Imaging 2018;48:1637-1647.

19. De Bernardi, Buda A, Guerra L, et al. Radiomics of the primary tumour as a tool to improve (18)F-FDG-PET sensitivity in detecting nodal metastases in endometrial cancer. EJNMMI Res 2018;8:86.

20. Silverberg RJ, Kurman RJ, Nogales F. Tumors of the uterine corpus. In: Tavassoli FA, Devilee P eds. Tumours of the Breast and Female Genital Organs. World Health Organization Classification of Tumours. Pathology & Genetics. Lyon, France: IACR Press Inc, 2003:217-258.

21. Miles KA, Ganeshan B, Hayball MP. CT texture analysis using the filtration-histogram method: what do the measurements mean? Cancer Imaging 2013;13:400-406.

22. Ytre-Hauge S, Husby JA, Magnussen IJ, et al. Preoperative tumor size at MRI predicts deep myometrial invasion, lymph node metastases, and patient outcome in endometrial carcinomas. Int J Gynecol Cancer 2015;25:459-466.

23. Sandrasegaran K, Lin Y, Asare-Sawiri M, Taiyini T, Tann M. CT texture analysis of pancreatic cancer. Eur Radiol 2019;29:1067-1073.

24. Ganeshan B, Miles KA. Quantifying tumour heterogeneity with CT. Cancer Imaging 2013;13:140-149.

25. Miles KA, Ganeshan B, Hayball MP. CT texture analysis using the filtration-histogram method: what do the measurements mean? Cancer Imaging 2013;13:400-406.

26. Hayano K, Tian F, Kambadakone AR, et al. Texture Analysis of Non-Contrast-Enhanced Computed Tomography for Assessing Angiogenesis and Survival of Soft Tissue Sarcoma. J Comput Assist Tomogr 2015;39:607-612.

27. Smith AD, Gray MR, del Campo SM, et al. Predicting Overall Survival in Patients With Metastatic Melanoma on Antiangiogenic Therapy and RECIST Stable Disease on Initial Posttherapy Images Using CT Texture Analysis. AJR Am J Roentgenol 2015;205:W283-W293.

28. Lubner MG, Stabo N, Lubner SJ, et al. CT textural analysis of hepatic metastatic colorectal cancer: pre-treatment tumor heterogeneity correlates with pathology and clinical outcomes. Abdom Imaging 2015;40:2331-2337.

29. Ng F, Kozarski R, Ganeshan B, Goh V. Assessment of tumor heterogeneity by CT texture analysis: can the largest cross-sectional area be used as an alternative to whole tumor analysis? Eur J Radiol 2013;82:342-348.

Table 1
Univariable and multivariable logistic regression for prediction of deep myometrial invasion, cervical stroma invasion, lymph node metastases and high-risk histological subtype at surgical staging. The top ranked CT derived texture feature is included in each category.

		Univariable		Multivariable	
Dependent variable (based on surgical staging/pathology)	Predicting variable (covariates)	Unadjusted OR (95% CI)	p	Adjusted* OR (95% CI)	p
Deep myometrial invasion (pDMI) (n=153)	ceCT_Entropy6	6.7 (2.8-16.0)	**<0.001**	3.7 (1.4-9.7)	**0.008**
	MRI tumour volume	1.04 (1.02-1.07)	**<0.001**	1.03 (1.00-1.05)	**0.02**
	MRI reading iDMI+	5.0 (2.5-10.0)	**<0.001**	2.3 (1.0-5.1)	**0.04**
	High-risk biopsy [a]	0.9 (0.5-1.9)	0.86	0.6 (0.2-1.4)	0.20
	Age	1.04 (1.00-1.07)	0.04	1.03 (0.99-1.07)	0.15
	Predictor with cutoff [b]				
(n=71/153)	ceCT_Entropy6 ≥4.84	3.9 (2.0-7.7)	**<0.001**	2.4 (1.1-5.2)	**0.02**
Cervical stroma invasion (pCSI) (n=153)	ceCT_Entropy6	4.4 (1.5-12.8)	0.006	3.9 (1.2-12.4)	**0.02**
	MRI tumour volume	1.01 (1.00-1.01)	0.15	1.00 (0.99-1.01)	0.73
	MRI reading iCSI+	4.9 (1.7-13.9)	0.003	3.8 (1.1-13.4)	**0.03**
	Biopsy Cervix+	2.0 (1.0-3.7)	0.04	2.1 (1.0-4.2)	**0.04**
	Age	1.02 (0.98-1.07)	0.27	1.02 (0.98-1.07)	0.37
	Predictor with cutoff [b]				
(n=68/153)	ceCT_Entropy6 ≥4.85	4.6 (1.8-11.8)	**0.001**	4.5 (1.6-12.6)	**0.004**
Lymph node metastases (pLNM) (n=131)	ceCT_Kurtosis5	1.3 (1.1-1.7)	0.01	1.1 (0.8-1.5)	0.75
	MRI tumour volume	1.02 (1.01-1.03)	0.005	1.02 (1.00-1.03)	0.06
	MRI reading iLNM+	21.6 (5.3-87.9)	**<0.001**	12.2 (2.5-59.0)	**0.002**
	High-risk biopsy [a]	3.4 (1.2-9.9)	0.03	1.8 (0.5-6.4)	0.38
	Age	1.02 (0.97-1.08)	0.41	1.00 (0.93-1.07)	0.90
	Predictor with cutoff [b]				
(n=61/131)	ceCT_Kurtosis5 >0.16	6.0 (1.6-22.4)	0.007	3.4 (0.8-14.0)	0.09
High-risk histological subtype [a] (n=153)	ceCT_MPP5	1.01 (1.00-1.03)	0.02	1.01 (1.00-1.03)	0.10
	MRI tumour volume	1.02 (1.01-1.03)	0.004	1.02 (1.00-1.03)	**0.05**
	High-risk biopsy [a]	30.2 (10.6-85.5)	**<0.001**	29.4 (10.0-86.4)	**<0.001**
	Age	1.02 (0.99-1.06)	0.21	1.00 (0.96-1.05)	0.96
	Predictor with cutoff [b]				
(n=96/153)	ceCT_MPP5 >24.2	4.7 (2.2-10.2)	**<0.001**	3.7 (1.3-10.1)	**0.01**

[a] High-risk-histological subtype is defined as endometrioid grade 3 or non-endometrioid subtype as opposed to low-risk histological subtype defined as endometrioid grade 1 and 2.

[b] Cutoffs are determined by ROC curve analysis selecting the highest Youden index. Multivariable analyses are identical except texture variables are now categorical.

* All covariates listed behind each dependent variable, grouped by vertical leaders, are included in each multivariable analysis. (When analysing texture variables with cutoff, the continuous variable is replaced by the corresponding categorical variable in the same analysis.)

Significant p values ($p<0.0025$ in univariable analyses (after correction for number of test variables and inter-variable correlations) and $p<0.05$ in multivariable analyses) are given in **bold.**

Texture features are annotated with number indicating spatial scale filter (SSF).

ceCT, contrast-enhanced CT; CI, confidence interval; CT, computed tomography; iCSI, imaging-assessed cervical stroma invasion; iDMI, imaging-assessed deep myometrial invasion; iLNM, imaging-assessed lymph node metastases; MPP, mean of positive pixels; MRI, magnetic resonance imaging; OR, odds ratio; pCSI, pathology-assessed cervical stroma invasion; pDMI, pathology-assessed deep myometrial invasion; pLNM, pathology-assessed lymph node metastases.

Table 2
Univariable and multivariable Cox regression analysis for prediction of recurrence- and progression-free survival after treatment for endometrial cancer (n=155).

		Univariable		Multivariable	
Outcome	Predictor	Unadjusted HR (95% CI)	p	Adjusted HR (95% CI)	p
RPFS	ceCT_Kurtosis5	1.2 (1.1-1.2)	**<0.001**	1.1 (1.0-1.2)	0.06
	MRI tumour volume	1.01 (1.00-1.01)	**<0.001**	1.01 (1.00-1.01)	**0.01**
	High-risk biopsy [a]	3.6 (1.9-6.9)	**<0.001**	2.6 (1.3-5.2)	**0.01**
	Age	1.03 (1.00-1.07)	0.06	1.02 (0.98-1.05)	0.33

[a] Categorical variable. High-risk biopsy is defined as endometrioid grade 3 or non-endometrioid subtype as opposed to low-risk comprising endometrioid grade 1 and 2.

Significant p values ($p<0.0025$ in univariable analyses (after correction for number of test variables and inter-variable correlations) and $p<0.05$ in multivariable analyses) are given in **bold**.

The texture feature (ceCT_Kurtosis5) is annotated with a number indicating spatial scale filter (SSF=5).

ceCT, contrast-enhanced CT; CI, confidence interval; CT, computed tomography; HR, hazard ratio; MRI, magnetic resonance imaging; RPFS, recurrence- and progression-free survival.

Figure legends

Figure 1

Endometrial carcinoma manually segmented (blue line) on contrast-enhanced CT image in (a) an 81-year-old woman diagnosed with stage 1a cancer (endometrioid grade 1). Texture analysis showed low tumour entropy (Entropy6=4.49 corresponding to 25-percentile in study cohort). (b) An 88-year-old woman with stage 2 cancer (endometrioid grade 1) and high tumour entropy (Entropy6=5.54 corresponding to 95-percentile). Native image on top and fine, medium and coarse filtration of the tumour depicted below.

Figure 2

Receiver operator characteristics (ROC)-curves visualising the diagnostic performance of the top ranked texture features for predicting presence of the staging parameters deep myometrial invasion (pDMI) (a), cervical stroma invasion (pCSI) (b), lymph node metastases (pLNM) (c) and for high-risk histological subtype (d). P values refer to the test of equal areas under the diagonal and the ROC-curve. AUC, area under the ROC-curve.

Figure 3

Kaplan-Meier plot depicting significantly different patient survival for the top ranked tumour texture feature Kurtosis5. High tumour values for Kurtosis5 (above 75-percentile) were significantly associated with reduced recurrence- and progression free survival ($p<0.001$). P value refers to the Mantel-Cox (log-rank) test.

Suppl. Figure 1A

Corresponding MR images (a-e) and tumour segmented CT image (f) in an 81-year-old woman diagnosed with stage 1a cancer (endometrioid grade 1) (same patient as in Figure 1a): Sagittal T2, depicting MRI axial oblique plane (red line) and CT coronal plane (blue line) (a), axial oblique T2 (b), axial oblique contrast-enhanced T1 (c), DWI b1000 (d), ADC-map (e) and contrast-enhanced CT image with tumour delineation (blue line) (f). The coronal CT plane was the best approximation of a true cross-sectional tumour plane in this patient – due to the uterus being anteverted.

Suppl. Figure 1B

Corresponding MR images (a-e) and tumour segmented CT image (f) in an 88-year-old woman with stage 2 cancer (endometrioid grade 1) (same patient as in Figure 1b): Sagittal T2, depicting MRI axial oblique plane (red line) and CT axial plane (blue line) (a), axial oblique T2 (b), axial oblique contrast-enhanced T1 (c), DWI b1000 (d), ADC-map (e) and contrast-enhanced CT image with tumour delineation (blue line) (f). Notice that the axial CT plane was the best approximation of a true cross-sectional tumour plane, being almost identical to the slightly oblique MRI plane, in this patient with a neutrally positioned uterus.

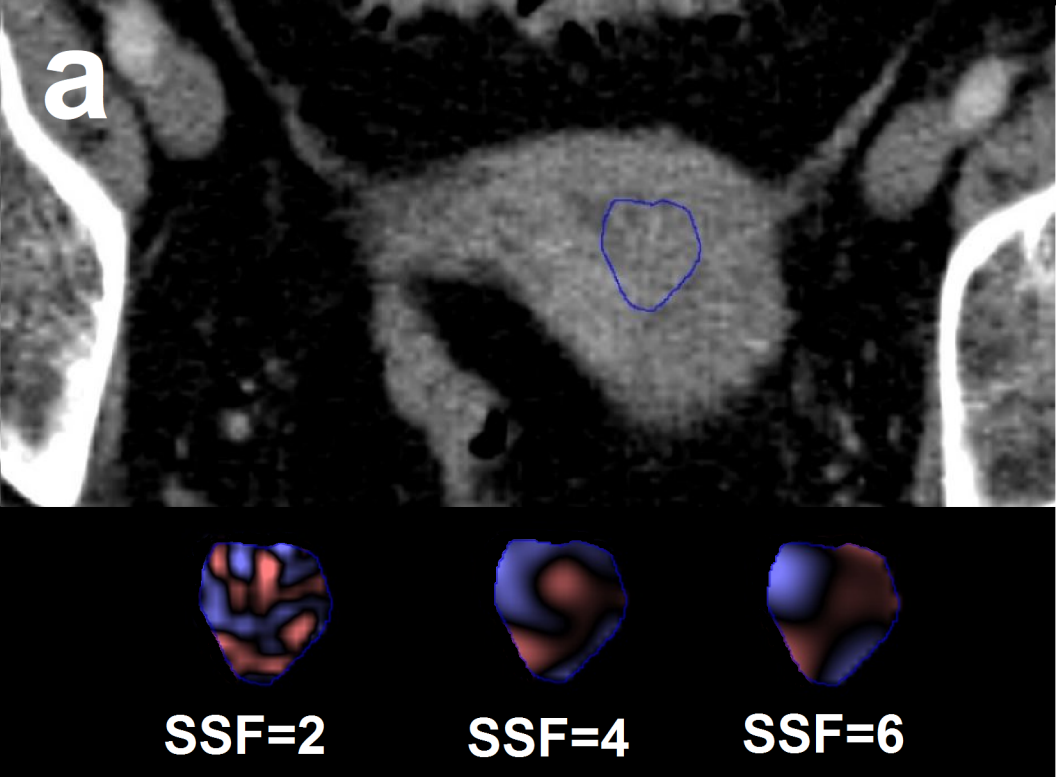
a
SSF=2
SSF=4
SSF=6

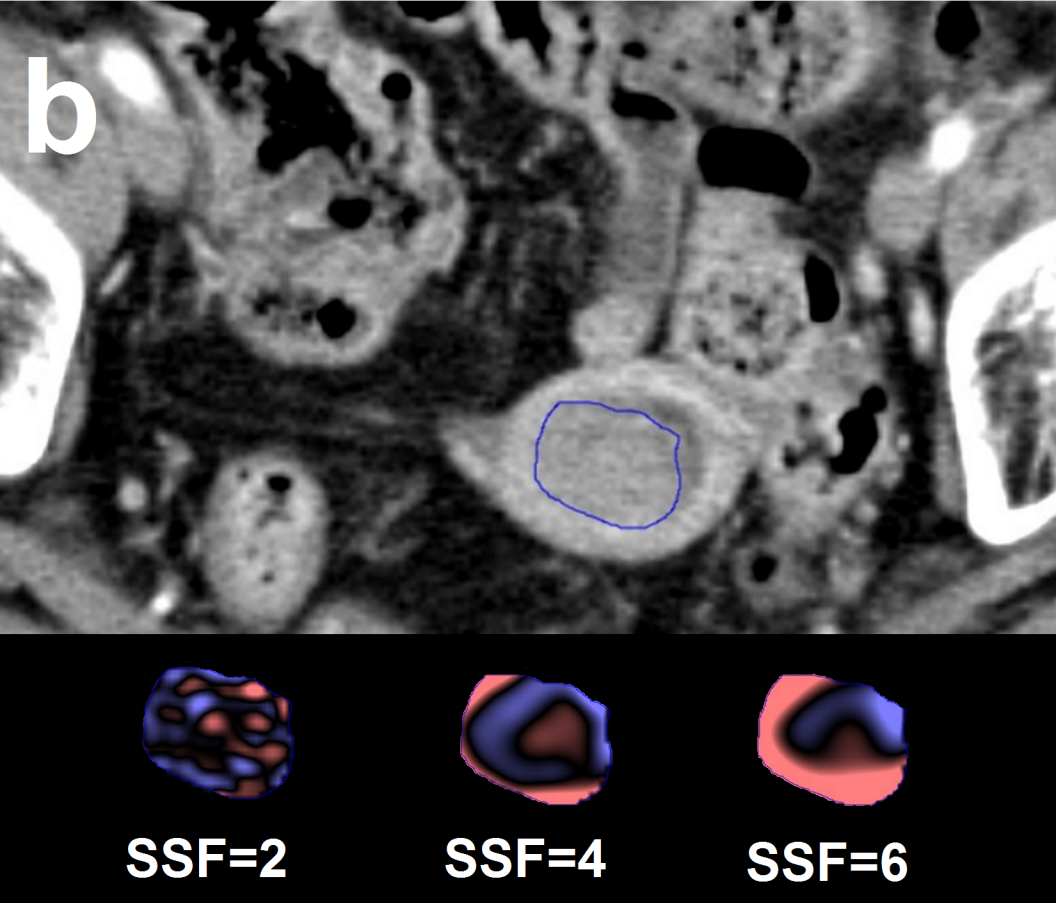
b
SSF=2
SSF=4
SSF=6

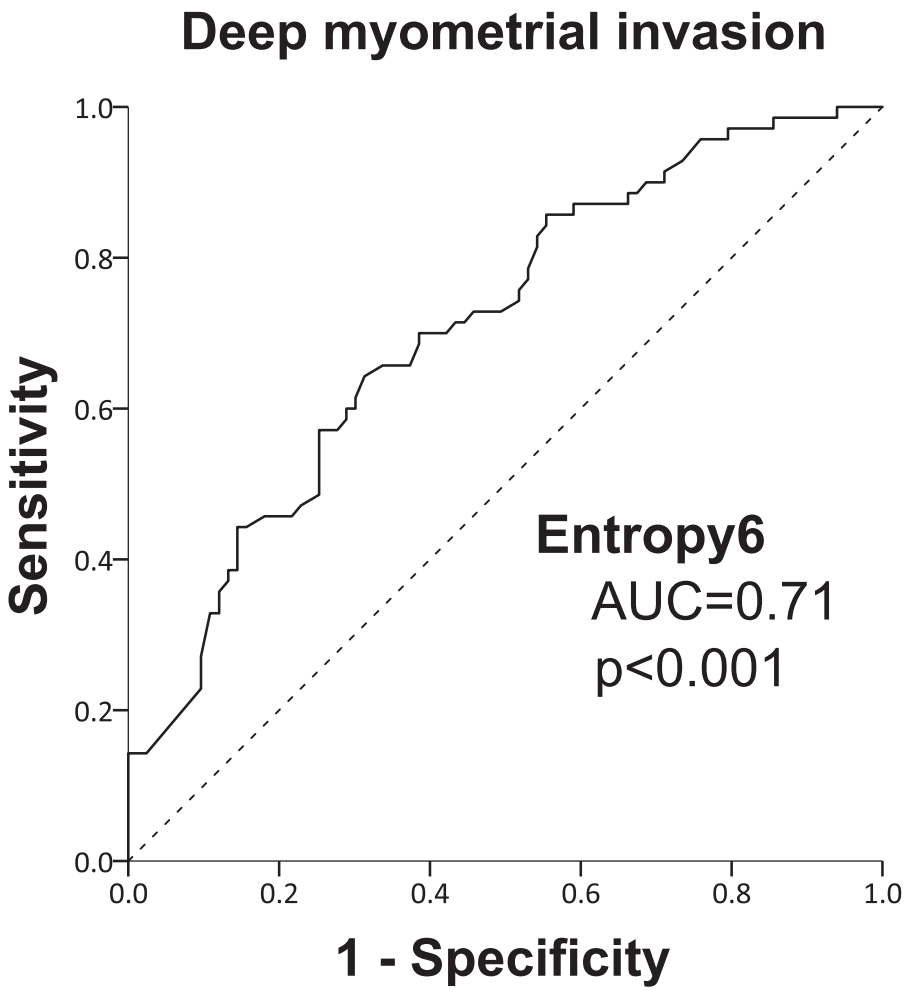
Deep myometrial invasion
Sensitivity
1.0
0.8
0.6
0.4
0.2
0.0
0.0
0.2
0.4
0.6
0.8
1.0
1 - Specificity
Entropy6
AUC=0.71
p<0.001

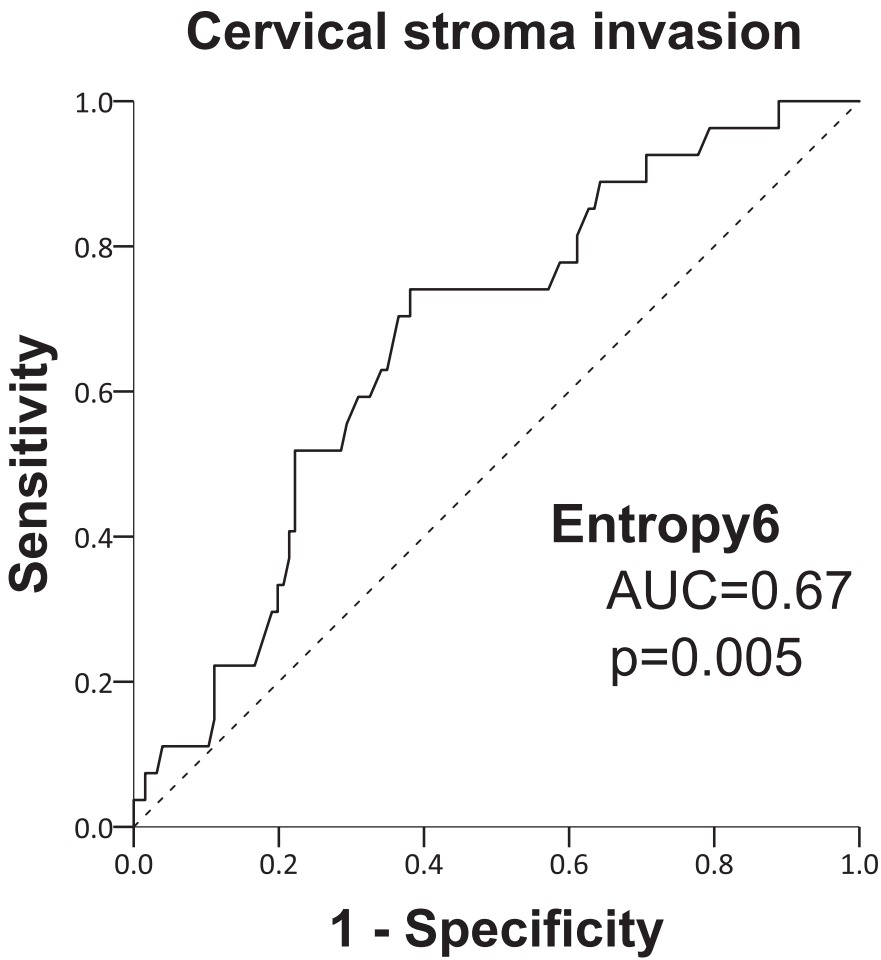
Cervical stroma invasion
Sensitivity
1 - Specificity
1.0
0.8
0.6
0.4
0.2
0.0
0.0
0.2
0.4
0.6
0.8
1.0
Entropy6
AUC=0.67
p=0.005

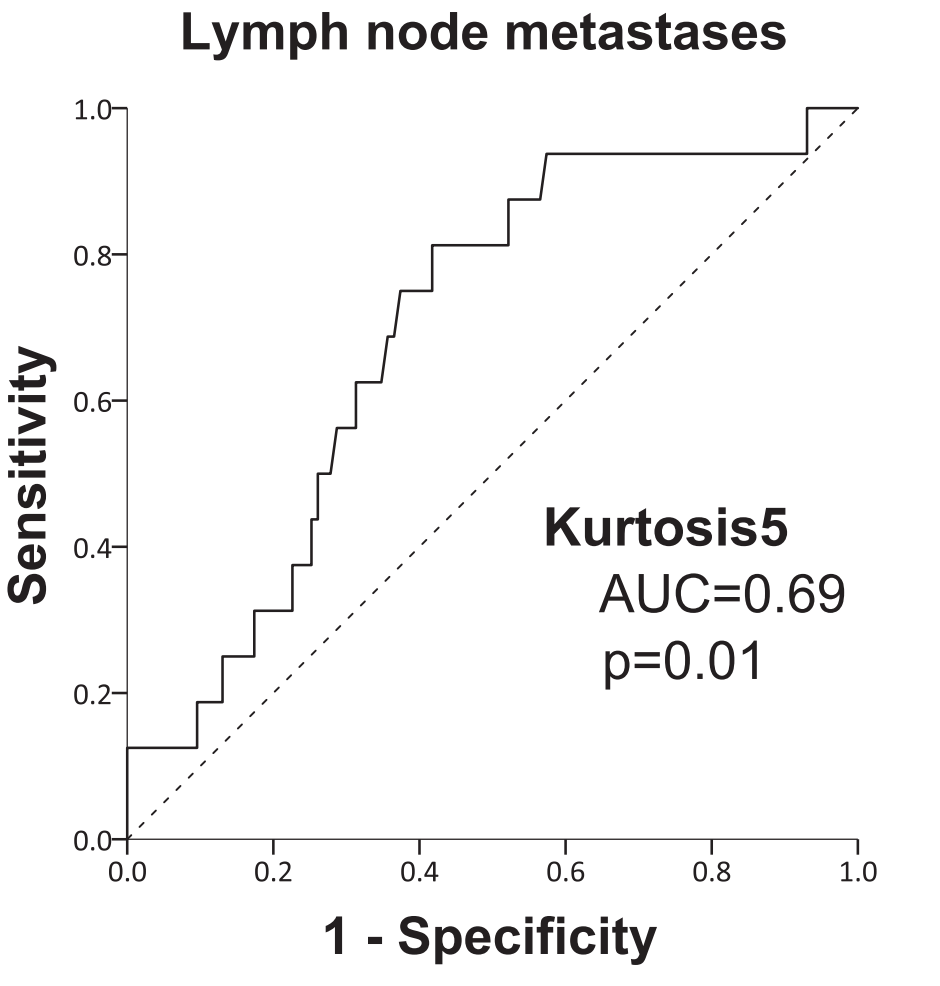
Lymph node metastases
Sensitivity
1 - Specificity
1.0
0.8
0.6
0.4
0.2
0.0
0.0
0.2
0.4
0.6
0.8
1.0
Kurtosis5
AUC=0.69
p=0.01

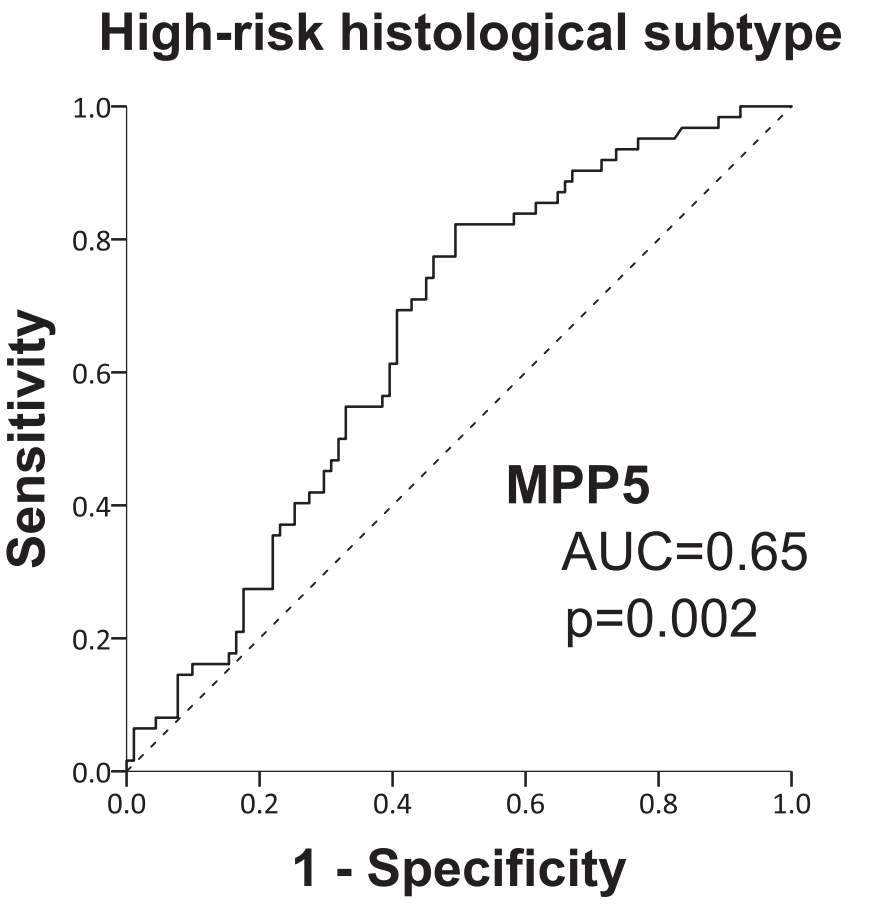
High-risk histological subtype
Sensitivity
1.0
0.8
0.6
0.4
0.2
0.0
0.0
0.2
0.4
0.6
0.8
1.0
1 - Specificity
MPP5
AUC=0.65
p=0.002

Kurtosis5

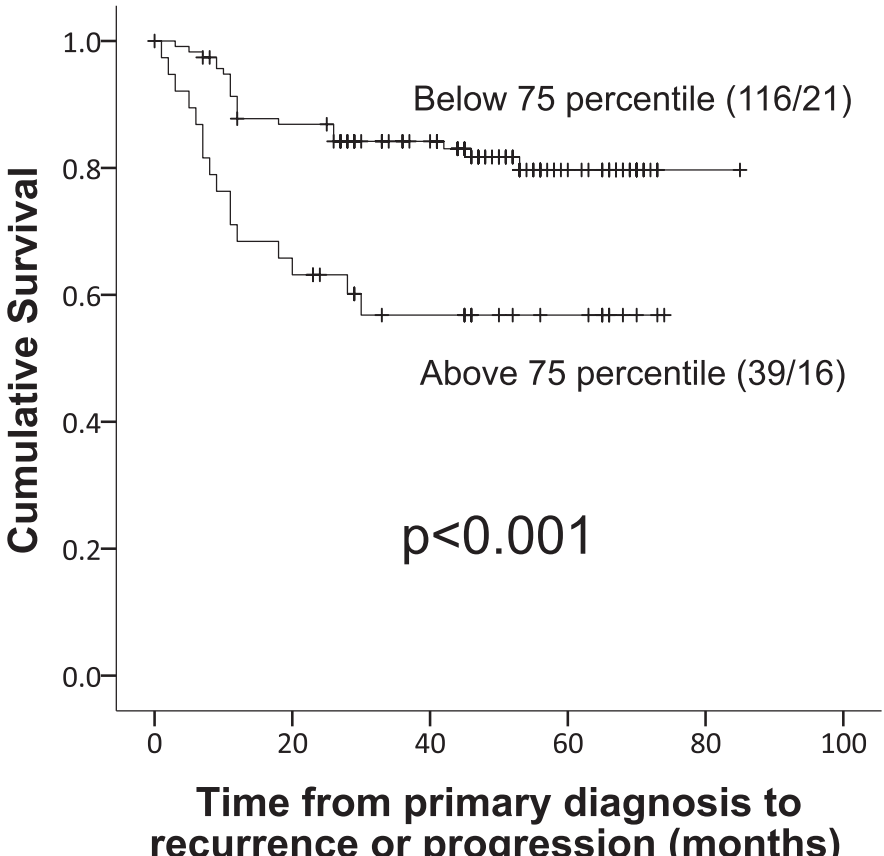
Cumulative Survival
1.0
0.8
0.6
0.4
0.2
0.0
Below 75 percentile (116/21)
Above 75 percentile (39/16)
p<0.001
0
20
40
60
80
100
Time from primary diagnosis to recurrence or progression (months)

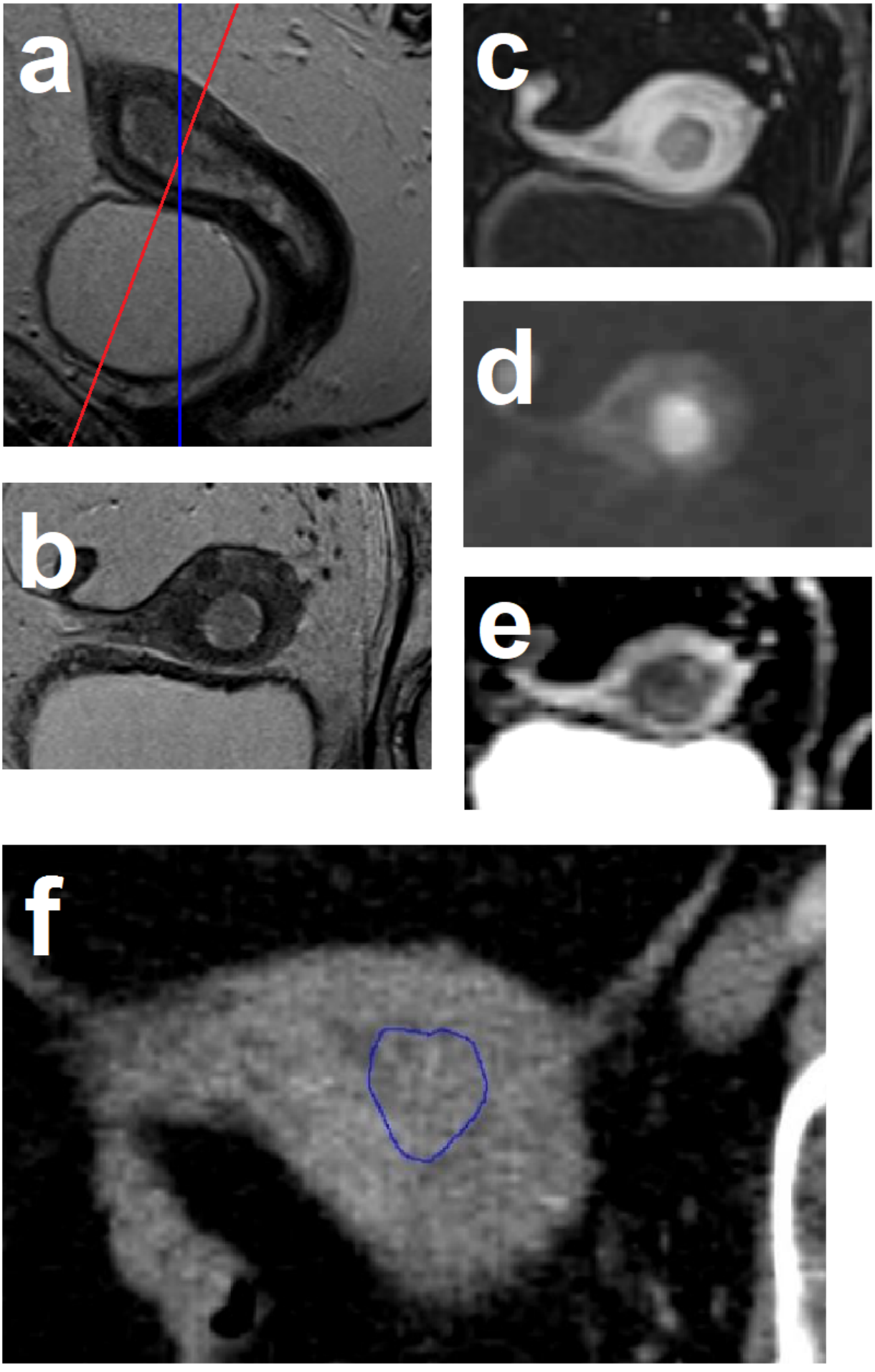
a
b
c
d
e
f

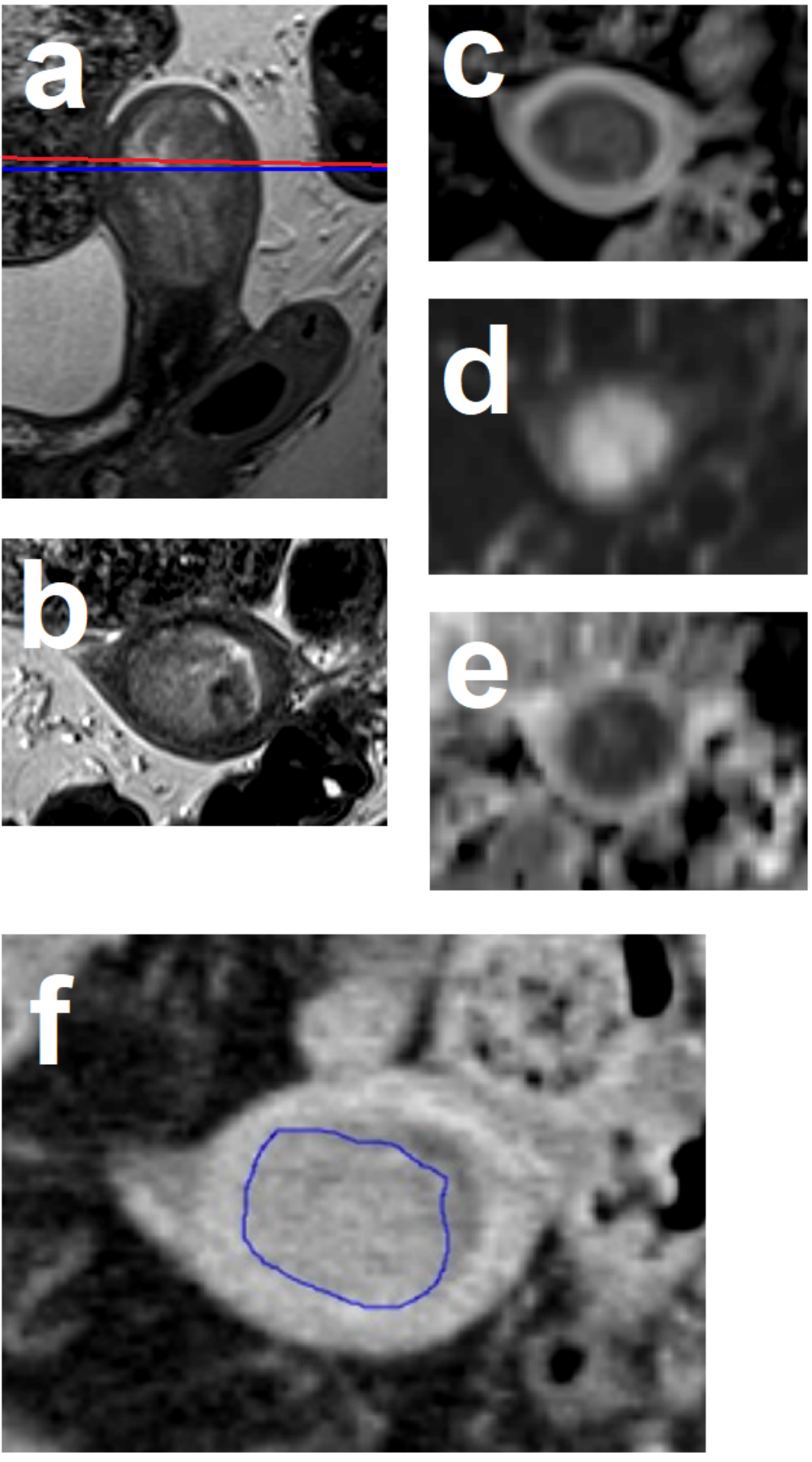
a
b
c
d
e
f

Suppl. Table 1
Spearman correlation coefficients (r_s) for CT derived texture features (at different filter levels (SSF 0-6)) in tumour ROIs of 155 endometrial cancer patients.

		Mean						SD						Entropy					
SSF		0	2	3	4	5	6	0	2	3	4	5	6	0	2	3	4	5	6
0																			
2	r_s	0.14						0.74 **						0.85 **					
3	r_s	0.21 *	0.97 **					0.44 **	0.70 **					0.70 **	0.88 **				
4	r_s	0.26 **	0.90 **	0.97 **				0.30 **	0.44 **	0.89 **				0.58 **	0.74 **	0.94 **			
5	r_s	0.33 **	0.76 **	0.85 **	0.94 **			0.24 *	0.30 **	0.72 **	0.93 **			0.54 **	0.66 **	0.86 **	0.96 **		
6	r_s	0.35 **	0.62 **	0.72 **	0.84 **	0.96 **		0.20 *	0.23 *	0.60 **	0.80 **	0.94 **		0.53 **	0.63 **	0.81 **	0.91 **	0.98 **	

		MPP						Skewness						Kurtosis					
SSF		0	2	3	4	5	6	0	2	3	4	5	6	0	2	3	4	5	6
0																			
2	r_s	0.11						0.40 **						0.40 **					
3	r_s	0.28 **	0.72 **					0.39 **	0.63 **					0.37 **	0.65 **				
4	r_s	0.32 **	0.48 **	0.87 **				0.40 **	0.42 **	0.81 **				0.32 **	0.34 **	0.72 **			
5	r_s	0.38 **	0.34 **	0.69 **	0.90 **			0.41 **	0.29 **	0.54 **	0.84 **			0.33 **	0.26 **	0.44 **	0.77 **		
6	r_s	0.41 **	0.28 **	0.58 **	0.78 **	0.95 **		0.38 **	0.23 **	0.38 **	0.63 **	0.91 **		0.31 **	0.25 **	0.31 **	0.49 **	0.84 **	

** Correlation is significant at the 0.0025 level (2-tailed).
* Correlation is significant at the 0.05 level (2-tailed).
CT, computed tomography; MPP, mean of positive pixels; ROI, region of interest; SD, standard deviation; SSF, spatial scale filter.

Suppl. Table 2
Top ranked CT derived texture features in relation to clinical and histological characteristics of 155 endometrial cancer patients.

		Entropy6 [a]		MPP5 [b]		Kurtosis5 [c]	
Variable	n	Median (95% CI)	p*	Median (95% CI)	p*	Median (95% CI)	p*
Myometrial invasion			**<0.001**		**<0.001**		**<0.001**
<50%	83	4.7 (4.5-4.8)		24 (19-28)		-0.3 (-0.4-0.0)	
≥50% (pDMI)	70	5.0 (4.8-5.1)		36 (28-44)		0.3 (0.1-0.9)	
Cervical stroma invasion			0.005		0.03		0.71
No	126	4.8 (4.7-4.8)		26 (22-31)		0.0 (-0.2-0.2)	
Yes (pCSI)	27	5.1 (4.9-5.2)		34 (27-45)		0.2 (-0.6-1.4)	
Lymph node metastases			0.10		0.56		0.01
No	115	4.8 (4.7-4.9)		28 (25-34)		0.0 (-0.3-0.2)	
Yes (pLNM)	16	5.1 (4.7-5.3)		32 (18-57)		0.8 (0.2-2.1)	
Histological type/grade			0.007		**0.002**		0.02
E1+2	91	4.7 (4.6-4.8)		24 (20-31)		0.0 (-0.3-0.2)	
E3+NE	62	4.9 (4.8-5.1)		35 (29-44)		0.3 (-0.2-1.0)	
Age, years			0.30		0.008		0.16
<68	77	4.8 (4.6-4.9)		25 (20-31)		-0.1 (-0.3-0.2)	
≥68 (median and above)	78	4.8 (4.7-5.0)		35 (27-44)		0.3 (-0.2-0.8)	
BMI, kg/m^2			0.05		0.14		0.28
<25	45	5.0 (4.7-5.2)		33 (24-45)		0.3 (-0.1-0.8)	
≥25 (overweight)	107	4.8 (4.7-4.9)		28 (24-31)		0.0 (-0.3-0.2)	

* Mann-Whitney U Test.

[a] Highest ranked CT derived texture feature for prediction of myometrial invasion (pDMI) and cervical stroma invasion (pCSI).

[b] Highest ranked CT derived texture feature for prediction of histological type/grade.

[c] Highest ranked CT derived texture feature for prediction of lymph node metastases (pLNM) and recurrence- and progression-free survival.

Texture features are annotated with number indicating spatial scale filter (SSF).

Significant p values after correction for number of test variables and inter-variable correlations (<0.0025) are given in **bold**.

BMI, body mass index; CI, confidence interval; CT, computed tomography; E1-3, endometrioid grade 1-3; MPP, mean of positive pixels; NE, non-endometrioid; pCSI, pathology-assessed cervical stroma invasion; pDMI, pathology-assessed deep myometrial invasion; pLNM, pathology-assessed lymph node metastases.

Suppl. Table 3
Top ranked CT derived texture features for predicting FIGO staging parameters, histological tumour characteristics and survival in 155 endometrial cancer patients.

	Deep myometrial invasion (pDMI)		Cervical stroma invasion (pCSI)		Lymph node metastases (pLNM)		High-risk histology (E3+NE)		Reduced recurrence- and progression-free survival	
Rank	Texture feature	p*	Texture feature	p*	Texture feature	p*	Texture feature	p*	Texture feature	p⁺
1	Entropy6	**8.74×10^{-6}**	Entropy6	0.0053	Kurtosis5	0.0121	MPP5	**0.0016**	Kurtosis5	**1.44×10^{-6}**
2	Kurtosis3	**9.52×10^{-6}**	Entropy5	0.0075	Kurtosis4	0.0123	Entropy4	**0.0022**	Kurtosis4	**2.05×10^{-5}**
3	Kurtosis4	**1.97×10^{-5}**	Entropy4	0.0153	Kurtosis2	0.0149	Entropy5	0.0029	Kurtosis3	**1.80×10^{-5}**
4	Entropy5	**6.97×10^{-5}**	MPP4	0.0193	Kurtosis6	0.0192	Entropy3	0.0037	Kurtosis6	0.0067
5	Entropy2	**2.96×10^{-4}**	Skewness3	0.0344	Kurtosis3	0.0320	Entropy6	0.0068	Skewness3	0.0114
6	Kurtosis5	**2.99×10^{-4}**	MPP5	0.0346	Entropy2	0.0365	MPP6	0.0068	Entropy5	0.0114
7	MPP6	**3.54×10^{-4}**	SD5	0.0405	MPP0§	0.0415	MPP4	0.0109	Entropy6	0.0126
8	Mean5	**4.27×10^{-4}**	SD4	0.0417	Mean0§	0.0422	Skewness2	0.0117	Skewness4	0.0155
9	Mean6	**4.33×10^{-4}**	SD6	0.0424	Entropy5	0.0730	SD6	0.0128	Entropy4	0.0243
10	Kurtosis2	**4.48×10^{-4}**	MPP3	0.0476	Entropy0	0.0800	Skewness3	0.0185	Kurtosis2	0.0250

* Mann-Whitney U Test.

⁺ Univariable Cox regression analysis.

§ *Low* values of MPP0 and Mean0 predicted lymph node metastases. For all other texture features listed, *high* values predicted high-risk disease.

Significant p values after correction for number of test variables and inter-variable correlations (<0.0025) are given in **bold**.

Texture features are annotated with number indicating spatial scale filter (SSF).

ceCT, contrast-enhanced CT; CT, computed tomography; E3, endometrioid grade 3; FIGO, the International Federation of Gynecology and Obstetrics; MPP, mean of positive pixels; NE, non-endometrioid; pCSI, pathology-assessed cervical stroma invasion; pDMI, pathology-assessed deep myometrial invasion; pLNM, pathology-assessed lymph node metastases; SD, standard deviation.